Design and Commissioning of the IRIS

A Setup for Aircraft Vapour Compression Cycle-Based Environmental Control System Testing

Ascione, Federica; Head, Adam J.; Colonna, Piero; De Servi, Carlo

DOI
10.1115/GT2024-123714

Publication date
2024

Published in
Cycle Innovations

Citation (APA)
Ascione, F., Head, A. J., Colonna, P., & De Servi, C. (2024). Design and Commissioning of the IRIS: A Setup for Aircraft Vapour Compression Cycle-Based Environmental Control System Testing. In *Cycle Innovations* Article v005t06a006 (Proceedings of the ASME Turbo Expo; Vol. 5). The American Society of Mechanical Engineers (ASME). https://doi.org/10.1115/GT2024-123714

Proceedings of ASME Turbo Expo 2024
Turbomachinery Technical Conference and Exposition
GT2024
June 24-28, 2024, London, United Kingdom

GT2024-123714

DESIGN AND COMMISSIONING OF THE IRIS: A SETUP FOR AIRCRAFT VAPOUR COMPRESSION CYCLE-BASED ENVIRONMENTAL CONTROL SYSTEM TESTING

Federica Ascione[1], Adam J. Head[1], Piero Colonna[1], Carlo De Servi[1,2,*]

[1]Propulsion and Power, Delft University of Technology, Kluyverweg 1, Delft, 2629 HS, The Netherlands
[2]Energy Technology Unit, VITO, Boeretang 200, BE-2400, Mol, Belgium

ABSTRACT

The aircraft Environmental Control System (ECS) is the main consumer of non-propulsive energy, accounting for 3% *of the total energy consumption among all the aircraft subsystems. The ECS efficiency can be improved by recurring to an electrically-driven Vapour Compression Cycle (VCC) system for cabin cooling. This work documents the detailed design and the commissioning of a novel experimental test rig, called Inverse organic Rankine cycle Integrated System (IRIS). The setup has been conceived for testing the performance of VCC systems and some of their components for aircraft ECS applications in different operating conditions, and for validating the numerical models developed for systems and components simulations. The facility implements a single-stage compression refrigeration cycle with two test sections: a volumetric compressor testing setup and an air-cooled condenser test bed. The evaporator is heated by a glycol-water mixture, warmed up in an independent loop. The design working fluid is R-1233zd(E). The successful commissioning of the facility is documented by discussing the data recorded during steady-state operation at the design operating point, together with the operation of the setup during start-up and shut-down procedures. The system cooling capacity is equal to* $17.88 \pm 0.8\,\mathrm{kW}$*, which is slightly higher than the design value of* $15.5\,\mathrm{kW}$*. The difference has a positive effect on the system efficiency, which is* 4% *higher than the one calculated at design.*

Keywords: Aircraft Environmental Control System, Vapour Compression Cycle, IRIS setup, R-1233zd(E).

NOMENCLATURE

Acronyms

ACM	Air Cycle Machine
BoP	Balance of Plant
COP	Coefficient Of Performance [-]
DAQ&C	Data Acquisition and Control
ECS	Environmental Control System
GWP	Global Warming Potential
HCFO	Hydroclorofluoroolefins
HFC	Hydrofluorocarbons
ICAO	International Civil Aviation Organization
IRIS	Inverse organic Rankine cycle Integrated System
MEA	More Electric Aircraft
NBP	Normal Boiling Point [K]
ODP	Ozone Depletion Potential
PID	Proportional–Integral–Derivative
P&ID	Piping and Instrumentation Diagram
PLC	Programmable Logic Controller
VCC	Vapour Compression Cycle

Roman letters

c_p	Specific heat at constant pressure $[\mathrm{J \cdot (kg \cdot K)^{-1}}]$
M	Molar mass $[\mathrm{g \cdot m^{-1}}]$
$\dot{m}$	Mass flow rate $[\mathrm{kg \cdot s^{-1}}]$
p	Pressure [Pa]
$\dot{Q}$	Thermal power [W]
T	Temperature [K]
$\dot{V}$	Volumetric flow rate $[\mathrm{m^3 \cdot s^{-1}}]$
$\dot{W}$	Mechanical power [W]
x	Vapour quality [-]

Greek letters

σ	Molecular complexity [-]
ρ	Density $[\mathrm{kg \cdot m^{-3}}]$

Superscripts and subscripts

a	Airflow
c	Critical thermodynamic point
compr	Compressor
cond	Condenser
eva	Evaporator
g-w	Glycol-water flow
refr	Refrigerant
v	Saturated vapour

*Corresponding author: c.m.deservi@tudelft.nl

1. INTRODUCTION

In response to the global climate change emergency, the aviation sector is moving toward more sustainable energy solutions. At the COP28 UN Climate Change Conference, the International Civil Aviation Organization (ICAO) and its member states agreed on a strategy to facilitate the global scale-up in the development, production and deployment of sustainable aviation fuels and other aviation cleaner energies. The long-term environmental objective is twofold: the 50% reduction of international aviation CO_2 emissions by 2030, and the achievement of net-zero carbon emissions by 2050 [1]. Therefore, both the aviation industry and academia have oriented significant research efforts toward aircraft electrification to reduce global weight and specific fuel consumption. The next generation of aircraft begins with the More Electric Aircraft (MEA), where sub-systems are electrified. The aircraft non-propulsive systems count for 5% of the total specific fuel consumption, and their electrification may considerably enhance the aircraft performance. The Environmental Control System (ECS) is the auxiliary system responsible for cabin air pressurization, passengers thermal comfort and avionics thermal management. The traditional ECS is the pneumatically-driven Air Cycle Machine (ACM). Novel ECS architectures have been investigated to improve the system efficiency, i.e., the bleed-less ACM [2]. Another option is the electrically-driven Vapour Compression Cycle (VCC) system, based on the inverse Rankine cycle technology. Its efficiency can be twofold the one of the ACM, independently from the aircraft flying condition, and it guarantees high cooling capacity even at ground operating conditions. Despite the large number of numerical works concerning the design and optimization of novel sustainable aircraft ECS architectures, only a few examples of experimental investigations are reported in the literature. Zaporozhets *et al.* [3] carried out an experimental study on the performance of a bootstrap ACM with high-pressure water separation. They simulated different flight conditions to evaluate the off-design performance and the dynamic response of the system to test its efficiency and reliability. Chowdhury *et al.* [4] document the design and realization of an experimental ground test facility reproducing the bleedless ACM of a Boeing 737-400. The system was tested to simulate various operating conditions. The outcome of the experimental campaign was used for validation purposes of the physics-based component models developed using commercial software [5]. An example of a VCC system for aircraft applications has been proposed by Mancin *et al.* [6]. They described a mini-VCC system for aircraft electronics thermal management. The system has a cooling capacity from 37 W to 374 W, and the working fluid is R-134a. The condenser is water-cooled, the piston compressor is oil-free, and a cold plate is used for the aeronautical electronic thermal management to meet the requirements of compactness and reliability.

To contribute to research on innovative systems and components for aircraft cabin air thermal management, a novel experimental test rig, called Inverse organic Rankine cycle Integrated System (IRIS), has been designed and commissioned at the Propulsion & Power Laboratory of the TU Delft Aerospace Engineering faculty. The setup has been conceived for testing the performance of VCC systems for aircraft ECS applications in different operating conditions, and for validating the *in-house* simulation and optimal design software for the VCC systems and components. The facility consists of a single Balance of Plant (BoP) which realizes a single-stage compression refrigeration cycle. It accommodates two test sections: a volumetric compressor testing setup and an air-cooled condenser test bed. The evaporator is heated by a glycol-water mixture, warmed up in an independent loop. An electronic expansion valve controls the degree of superheating of the refrigerant vapour at the compression suction port. The setup was designed with the low-Global Warming Potential (GWP) refrigerant R-1233zd(E) as the working fluid. This fluid is an alternative to the state-of-the-art R-134a refrigerant. Other working fluid, pure or mixture could be used in the future, with appropriate modifications to the setup. The system is designed for a cooling capacity of 15.5 kW.

This work documents the detailed design and the commissioning of the IRIS setup. First, the design requirements and the selection criteria of the system configuration and the working fluid are illustrated. Then, the choice of hardware, measurement instrumentation and control procedures is reported in relation to the objectives of the future experimental campaigns. Next, the commissioning of the facility is documented by discussing the data recorded during operation at steady-state at the design operating point, together with the operation of the setup during start-up and the shut-down procedures. The design operating condition corresponds to a temperature of evaporation equal to 20 °C, and a temperature lift between condensation and evaporation of 45 °C. The values of temperature and pressure are measured at all the relevant state points of the thermodynamic cycle, and the cycle Coefficient Of Performance (COP) is estimated. Finally, conclusions and future work are stated.

2. PRELIMINARY DESIGN

VCC systems are already state-of-the-art technology for helicopter cabin air cooling, therefore the idea underpinning the conceptualization of the IRIS setup is to design a simple and flexible facility in line with the requirements of this application. However, to comply with logistic constraints, the IRIS setup is characterized by two differences from the traditional helicopter ECS configuration: i) the absence of the intercooler in the BoP, ii) the utilization of a plate heat exchanger as the evaporator, whereas the refrigerant is warmed up by a mixture of 20% ethylene glycol and water, instead of air.

The helicopter ECS is normally sized for a critical operating condition, i.e., the helicopter is on the ground on a hot and humid day [7], and the design requirements of the IRIS setup comply with this specific case. The cooling duty of the system is 15.5 kW. The temperature of the environmental air entering the ram air duct is equal to 40 °C. In the refrigerant loop, the condensation temperature is a fixed value equal to 65 °C. The main driver of the system is a volumetric compressor, therefore, to allow for safe operation, the suction pressure must be higher than the atmospheric pressure.

The selection of the working fluid of the refrigeration loop is based on the findings from the preliminary design of the helicopter ECS reported in Ref. [8]. The authors developed a steady-state model of the VCC-based ECS using the acausal modelling language Modelica to assess the effect of the working fluid on the design feasibility and the thermodynamic performance of the system. A list of low-GWP refrigerants belonging to the class of the haloolefins and natural compounds has been tested, by optimizing the system COP as a function of the compressor interstage pressure. From the optimal values of system efficiency, the selected working fluids have been ranked to preliminarily identify the best alternative to the state-of-the-art R-134a. The results show that, compared to R-134a, the system efficiency significantly increases when using refrigerants belonging to the group of the haloolefins, i.e., R-1233zd(E), R-1336mzz(Z), R-1224yd(Z) and R-1234ze(Z), reaching a maximum enhancement of 15% in the case of R-1233zd(E). Based on the outcome of the numerical investigation, the refrigerant R-1233zd(E) has been selected as the design refrigerant for the IRIS setup. With reference to Tab. 1, the main properties of this working fluid, benchmarked against R-134a, can be summarized as i) higher molecular complexity σ; ii) larger molar mass M; iii) higher critical temperature and lower critical pressure; iv) significantly lower saturated vapour density. These characteristics allow for a reduction of the thermodynamic losses associated with the desuperheating at the compressor outlet, thus enhancing the system COP. Moreover, according to requirements stated in the Kigali amendment to the Montréal Protocol [9], R-1233zd(E) may be considered as an alternative working fluid to R-134a thanks to its excellent environmental properties.

TABLE 1: Thermodynamic and environmental properties of the IRIS design working fluid R-1233zd(E) as compared to R-134a [10].

Working fluid	R-1223zd(E)	R-134a
Refrigerant class	HCFO	HFC
T_c / °C	166.45	101.06
p_c / bar	36.24	40.49
NBP / °C	18.26	−26.37
M / g · m^{-1}	130.05	109.03
σ / -	3.92	−1.10
$\rho_{v,T=293.15K}$ / kg · m^{-3}	6.06	27.78
GWP[1]	5	1300
ODP	0	0
Safety group[2]	A1	A1

Similarly to what was done in the case of the study on the helicopter ECS preliminary design [8], a simplified zero-dimensional and steady-state model of the IRIS setup has been developed using the causal Modelica language. This model accounts for the pressure drops within the heat exchangers, and it neglects those occurring in the system piping. The design operating conditions of the R-1233zd(E) loop have been estimated for each state point of the thermodynamic cycle, resorting to a well-known commercial program [10]. Table 2 provides the calculated values of pressure and temperature at all the relevant thermodynamic state points for the refrigerant loop, together with the design specifications of its main components. The predicted design cooling duty of the setup in nominal conditions is 15.5 kW. The refrigerant mass flow rate is equal to 0.105 kg/s. The subcooling and the superheating degree are set to 5 K. The system simulations are performed considering an inlet temperature of the glycol-water stream in the evaporator of 45 °C at atmospheric pressure. The temperature decrease is equal to 10 K and the fluid volumetric flow rate is 1.30 m^3/h. On the condenser side, the inlet air is at a temperature of 40 °C at atmospheric pressure with a mass flow rate of 1.4 kg/s. The air outlet temperature is estimated to be equal to 54 °C. The predicted system COP is 3.60 .

[1]The authors refer to the index GWP_{100}, which estimates the environmental impact of a substance with respect to that of the CO_2 over a time horizon of 100 years.

[2]According to the ANSI/ASHRAE Standard 34 [11] refrigerant safety classification.

TABLE 2: Preliminary design specifications of the IRIS setup refrigeration loop. The state points refer to the P&ID in Fig. 1.

Refrigeration loop			
State point	***T* / °C**	***p* / bar**	***x* / -**
1	25	1.08	Superheated vapour
2≡3	80.18	4.48	Superheated vapour
4	60.76	4.45	Subcooled liquid
5	20	1.08	0.26

Refrigerant mass flow rate	$\dot{m}_{refr}$ / kg·s^{-1}	0.105
Evaporator heat duty	$\dot{Q}_{eva}$ / kW	15.5
Condenser heat duty	$\dot{Q}_{cond}$ / kW	19.8
Compressor power demand	$\dot{W}_{compr}$ / kW	4.30
COP	-	3.6

3. DETAILED DESIGN

Figure 1 shows the detailed Piping and Instrumentation Diagram (P&ID) of the facility. According to the ANSI/ISA standard 5.1 [12], the components and the instrumentation are identified by standardized symbols and tags. A complete legend of the abbreviations used for the section lines, the equipment and the instrumentation is reported in Fig. 1. The system includes three different fluid circuits hereinafter referred to as i) *heating loop*, providing thermal energy input to the evaporator, whose working fluid is a mixture of ethylene glycol and water; ii) *cooling loop*, a suction-type wind tunnel operating with air, for condenser testing; iii) *refrigeration loop*, namely the VCC system, whose working fluid is the refrigerant R-1233zd(E).

Figure 2 shows three-dimensional CAD drawings of the IRIS setup. The heating and the refrigeration loop of the IRIS setup are installed in an independent room, where the components are mounted on an aluminium frame, thus realizing a compact layout (Fig. 2a). The cooling loop is located outside the room in a L-shaped structure that houses a wind tunnel (Fig. 2a). A fan positioned at the exit port sucks in ambient air. The condenser is installed inside the tunnel and connected with the rest of the refrigeration loop located in the cabinet via two hoses. The external structure is designed to protect the components of the wind tunnel and it features several removable panels that provide easy access to components and instrumentation of the loop for maintenance, replacement or to add further measurement sensors to the condenser test section (Fig. 2b).

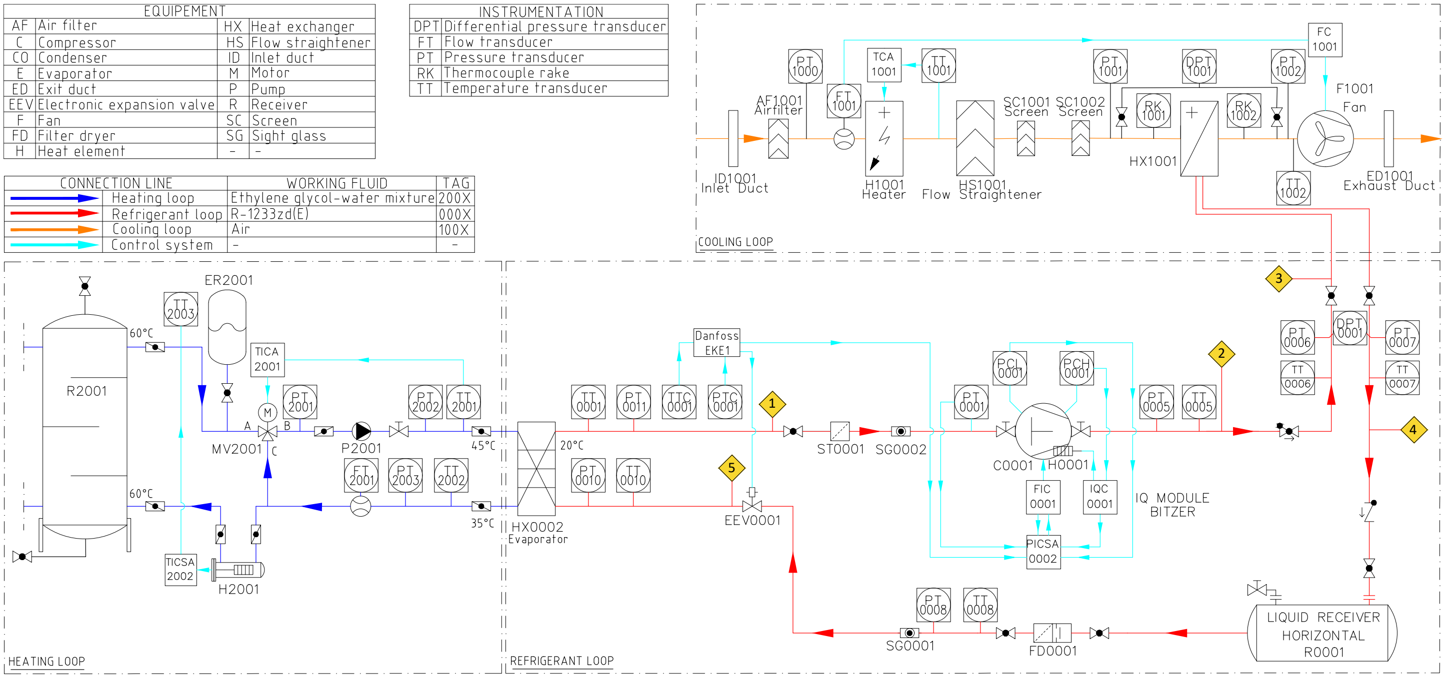

FIGURE 1: Piping and Instrumentation Diagram (P&ID) of the IRIS setup.

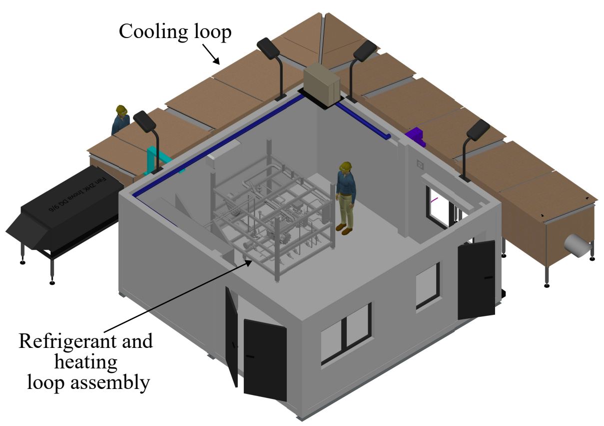

(a) Isometric view of the IRIS showing the refrigeration and heating loops within the laboratory room.

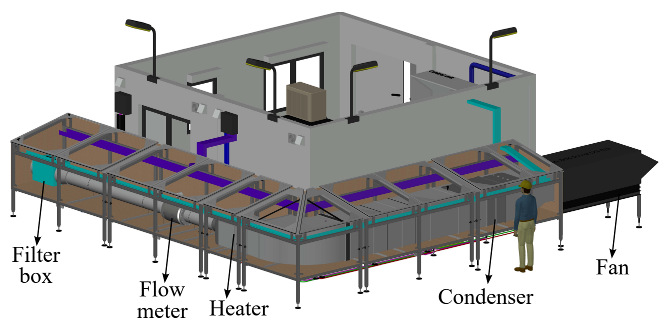

(b) Isometric view of the cooling loop L-shaped wind tunnel.

FIGURE 2: Three-dimensional CAD drawings of the IRIS setup layout.

3.1 Heating Loop

The heating loop serves as the continuous thermal energy source for the refrigerant within the evaporator (HX0002 in Fig. 1). The working fluid is an antifreeze, a mixture of 20% ethylene glycol and 80% water. The fluid is stored in an insulated tank with a capacity of 300 l. The hot fluid is circulated by a constant rotational speed pump (P2001). During the warming up of the loop, the three-way mixing valve (MV2001) is fully open in position A-B, thus the glycol-water mixture flows only through the evaporator. Upon returning to the tank, the electric heater (H2001) warms up the fluid until the working fluid temperature at the evaporator inlet reaches a given set-point value. Then, the electric heater is turned off, and the water temperature at the evaporator inlet is kept constant by controlling the glycol-water mass flow rate directed from the tank to the evaporator through the mixing valve. The mixing valve allows for the recirculation of a part of the fluid from the outlet of the evaporator (C) with the hot fluid stream from the tank (A). This allows to regulate the temperature in the evaporator, independently from the heater. Finally, to protect the loop from pressure buildup which may be caused by an increase in the water temperature, an expansion receiver (ER2001) is positioned downstream of the tank. The nominal diameter of the hoses of the heating loop is 22 mm, and they are insulated with polyethylene foam sleeves.

3.2 Cooling loop

In the cooling loop, air is used to cool down and liquefy the refrigerant flow within the condenser (HX1001 in Fig. 1). In the same fashion as a suction-type wind tunnel, the fan (F1001) is located downstream of the test section to suck the environmental air. At the tunnel inlet section, there is a box hosting a fibreglass filter (AF1001) keeping the incoming air free of any pollutants. To comply with the design specifications, an electric air heater (H1001) is installed upstream of the test section to increase the air stream temperature entering the condenser (HX1001) up to a set point value. A flow straightener (HS1001) and two screens (SC1001 and SC1002) are located upstream of the condenser to promote flow uniformity. To guarantee good reliability of the measurements, the ANSI/ASHRAE Standard 41.2-2022 [13] prescribes that the length of the duct between the flow straighteners and the test section should be at least equal to the so-called *development length* of five times the hydraulic diameter of the test section. In the cooling loop, the test section is the condenser itself, whose frontal dimensions on the air side are $0.79\,\mathrm{m} \times 0.71\,\mathrm{m}$, thus a distance of approximately 4 m separates the flow straighteners and the condenser. The condenser is currently a microchannel heat exchanger with multilouvered fins on the air side. A variable-speed centrifugal fan (F1001) is situated upstream of the exhaust duct (ED1001). The exit door incorporates movable buffers which open when the setup operations are started.

3.3 Refrigerant Loop

The refrigerant loop is a single compression stage VCC system. The evaporator (HX0002 in Fig. 1) is a brazed plate heat exchanger with a countercurrent flow arrangement. The refrigerant, warmed up by the glycol-water mixture flow, evaporates and reaches a superheated vapour state upstream of the compressor (C0001). This is the semi-hermetic ECOLINE 4HE-18Y-40P reciprocating compressor manufactured by *Bitzer*. The internal kinematics are lubricated with the BSE55 polyolester oil. The machine is driven by an electric motor with a maximum input power of 22 kW, and it features an external frequency inverter. The compressor is equipped with an integrated IQ (in-phase/quadrature) module which is used for high-pressure switch, data log, alarm history and Modbus RTU communication. Downstream of the compressor, the superheated refrigerant enters the condenser, where it undergoes the processes of desuperheating, condensation and subcooling due to the effect of the air of the cooling loop. The condensate enters the receiver (R0001), where the refrigerant charge is stored. This component is followed by the filter drier (FD0001) and the sight glass (SG0001). The filter drier is used to trap coarse particulate or any copper shavings and to capture any moisture dissolved in the fluid. The sight glass is an optical access to check whether there are any gas bubbles in the fluid, which would indicate that the refrigerant charge is low. Downstream the receiver, the refrigerant is expanded back to the evaporation pressure by means of the electronic expansion valve (EEV0001), equipped with a *Danfoss EKE1* superheat controller. This device regulates the refrigerant charge delivered to the evaporator to maintain the proper superheating degree and to prevent even a small amount of liquid from being ingested by the reciprocating compressor, thus causing its failure. A sight glass (SG0002) is installed upstream of the compressor suction port, providing optical access to this critical section of the loop. Polyethylene foam sleeves cover all the piping for thermal insulation.

4. INSTRUMENTATION, DATA ACQUISITION AND CONTROL

A data acquisition and control (DAQ&C) system is used to acquire and record data from the sensors and to control the system by delivering appropriate signals to the various actuators. The core of the DAQ&C system is the *National Instrument* (NI) compactRIO (cRIO) 9056 controller, which can accommodate a maximum of eight NI input/output (I/O) modules, handling digital or analog signals. In addition, the Modbus communication protocol is used for the *Danfoss* EKE 1C superheat controller and for the *Bitzer* compressor IQ module. Table 3 lists the characteristics of the modules hosted in the cRIO-9056 and the hardware connected to each of them. The DAQ&C is connected to a computer via an Ethernet link and runs the *IRIS software* LabView program. The software features a graphical user interface allowing the operator to easily monitor, control and record the process variables in real-time.

4.1 Instrumentation

The heating loop is equipped with three temperature and pressure transducers (Fig. 1). Each transducer transmits a 4 - 20 mA output signal to the module NI-9208 of the cRIO-9056. The glycol-water volumetric flow rate circulating within the loop is monitored with an electromagnetic flow meter (FT2001 in Fig. 1) located downstream of the evaporator (HX0002). The measured value of flow rate is transmitted via a 4 - 20 mA output signal to a NI-9208 A/D input module of the cRIO-9056 controller.

The cooling loop is instrumented with three pressure transducers and two temperature transducers (Fig. 1). Each pressure and temperature sensor transmits a 4 - 20 mA signal to the NI-9208 module of the cRIO-9056 controller. A differential pressure transducer (DPT1001) monitors the airflow pressure drop across the condenser test section. The air volumetric flow rate is measured via the ultrasonic flow meter (FT1001). This device is directly connected to a temperature and a pressure sensor, which provide the process measurements needed for the calculation of the corrected volumetric flow rate. All these pieces of equipment provide a 4 - 20 mA output analog signal to the cRIO-9056 controller. Finally, according to the current design of the IRIS setup, in the near future, two thermocouple rakes will be installed at the inlet and at the outlet section of the condenser test section to measure the airflow temperature distribution. These frames have been designed to accommodate 9 and 20 thermocouples, respectively.

The refrigerant loop is equipped with six temperature and pressure transducers, located in the most significant sections of the loop to allow for the system and the components energy balances, i.e., in the proximity of the inlet and the outlet ports of each main component (Fig. 1). A differential pressure transducer (DPT0001) measures the pressure drop of the refrigerant flow across the

TABLE 3: List of modules equipping the NI cRIO-9056 controller.

Model	Quantity	Type	Range	Channels	Description
Analog					
NI-9208	3	Current input	4 - 20 mA	16	Temperature, pressure and flow transmitters
NI-9264	1	Voltage output	0 - 10 V	16	Compressor frequency control, air heater control, mixing valve control
NI-9202	1	Voltage input	0 - 10 V	16	Differential pressure transducer, mixing valve actuator
Digital					
NI-9375	1	Input/Output	-	32	Alarms, pump enable, air heater enable, water heater enable, fan enable
Thermocouple					
NI-9214	2	Thermocouple type T	-	16	Thermocouple rake

condenser. All sensors output a 4 - 20 mA signal to the NI-9208 A/D input module of the cRIO-9056 controller.

Table 4 lists all the relevant data about the instrumentation installed in the IRIS setup.

4.2 Control strategy

To ensure the correct and safe functionality of the IRIS setup during the start-up, operation and shut-down procedures, six control loops have been implemented (Fig. 1).

The refrigerant loop is controlled by two loops, i.e., with reference to the P&ID in Fig. 1, the superheat controller (SHC0001) and the pressure controller (PICSA0002). The SHC0001 control loop sets the superheating degree at the evaporator outlet to prevent any liquid droplet from reaching the compressor suction port. This is achieved by regulating the opening of the EEV0001 valve. The controller hardware includes: i) a pressure sensor (PTC0001) to measure the evaporation pressure, ii) a temperature sensor (TIC0001) to monitor the refrigerant temperature at the evaporator outlet, iii) the expansion valve (EEV0001), iv) the *Danfoss* EKE 1C controller, v) a *Danfoss* EKE 2U power supply for backup purposes. A control algorithm is programmed in the firmware of the *Danfoss* EKE 1C controller, where both the temperature and the pressure sensors are directly wired. The EKE 1C unit determines the value of the superheating degree as a difference between the temperature measured at the outlet of the heat exchanger and the saturation temperature at the evaporation pressure. The controller regulates the opening of the EEV0001 expansion valve to match the calculated degree of superheating with a given set point value. During the commissioning of the setup, this controller has been configured to automatically calculate the minimum stable set point of superheating degree within an operating range provided by the operator. The PICSA0002 control loop sets the compressor suction pressure (PT0001) by varying the rotational speed of the compressor via the *Bitzer* Varypack frequency inverter (FIC0001). This control algorithm, a proportional–integral–derivative (PID) feedback, is implemented in the programmable logic controller (PLC). The purpose of this control loop is to prevent subatmospheric inlet conditions, which can cause damage to the compressor components. In the event that the pressure at the compressor inlet is too low during operation, a low-pressure switch (PCL0001) is triggered, causing an immediate shut-down of the loop. Additionally, the compressor IQ module is connected to a high-pressure switch (PCH0001) to protect the compressor from any pressure overshoot.

In the cooling loop, the TCA1001 control loop regulates the airflow temperature entering the condenser (TT1001). This control is implemented in the PLC and it is based on a PID control logic. The heater (H1001) is composed of four heating elements with a power capacity of 17 kW each. During operation, the heating power of the first element can be regulated, while the other three can only be turned on or off. The cooling loop includes also an air flow rate controller, directly implemented in the PLC using a PID feedback mechanism. This control system regulates the fan (FC1001) rotational speed to tune the air mass flow rate to a specific set point value.

In the heating loop, there are two temperature control systems, namely, TICSA2002 and TICA2001. The TICSA2002 control loop is implemented in the PLC, and it is based on an on/off control logic. If the temperature TT2003 falls below a set point value, the heater turns on. The TICA2001 controller, integrated into the PLC, leverages a PID control logic and it is active only during the operation of the refrigerant loop. The goal is to keep the glycol-water temperature at the evaporator inlet constant by regulating the opening of the MV2001 three-way mixing valve. During start-up, the valve operates in position A-B, and the working fluid flows from the receiver to the evaporator. During operation, to keep the glycol-water temperature constant at the evaporator inlet, a part of the colder fluid from the evaporator outlet is recirculated into the port C of the valve to be mixed with the hot fluid from the tank. The valve opening is regulated based on the offset between the set point and the process value of the temperature TT2001.

In addition to the control loops described thus far, other process variables are monitored and can trigger warnings, alarms or emergency shutdowns, depending on the event severity.

5. COMMISSIONING

Before the refrigerant is charged in the IRIS setup, a pressure and leakage test was successfully performed following the guidelines of the standard DIN EN 378-2 [14]. This safety procedure is used to prove the leak tightness of the components. The test is performed using dry nitrogen, an odourless and inert gas. An electronic device is used to detect any gas leakages. The low-pressure and the high-pressure lines are tested separately with a maximum pressure of 8 bar and 15 bar, respectively. For each test, the loop hoses were filled in with nitrogen, and the pressure was increased to the strength test value and held for 15 minutes. After the successful completion of the leakage test, the refrigerant loop has been filled with 6.7 kg of R-1233zd(E). Approximately 300 l

TABLE 4: Specifications of the process sensors equipping the IRIS setup.

Loop	Property	Tag	Model	Signal	Range	Accuracy (Type B)
Heating loop	Temperature	TT2001, TT2002, TT2003	*WIKA* TR21-B	4 - 20 mA	0... + 150 °C	Class A + ±0.25 K
	Pressure	PT2001	*WIKA* S-20	4 - 20 mA	−1... + 5 bar(g)	±0.25% of span
	Pressure	PT2002, PT2003	*WIKA* S-20	4 - 20 mA	0... + 4 bar(g)	±0.25% of span
	Flow rate	FT2001	*Endress+Hauser* Proline Promag W 400	4 - 20 mA	0...75 dm^3/min	±0.5%
Cooling loop	Temperature	TT1001, TT1002	*WIKA* TR36	4 - 20 mA	0... + 150 °C	Class A + ±0.25 K
	Pressure	PT1000	*WIKA* S-20	4 - 20 mA	−300... + 300 mbar(g)	±0.25% of span
	Pressure	PT1001, PT1002	*WIKA* S-20	4 - 20 mA	−500... + 500 mbar(g)	±0.25% of span
	Differential pressure	DPT1001	*Siemens* QBM4100-1U	4 - 20 mA	−50... + 50 mbar	±3% full scale
	Flow rate	FT1001	*KROHNE* Optisonic 7300	4 - 20 mA	0.4...1.4 kg/s	±1.5%
	Temperature	-	*KROHNE* Optitemp TRA-P10	4 - 20 mA	0...100 °C	±0.1% of span
	Pressure	-	*KROHNE* Optibar PM 3050	4 - 20 mA	0...0.4 bar	±0.2%
Refrigerant loop	Temperature	TT0001-TT0008	*WIKA* TR21-B	4 - 20 mA	0... + 150 °C	Class A + ±0.25 K
	Temperature	TT0010	*WIKA* TR21-B	4 - 20 mA	−10... + 150 °C	Class A + ±0.25 K
	Pressure	PT0001, PT0010	*WIKA* S-20	4 - 20 mA	−1... + 0.6 bar(g)	±0.25% of span
	Pressure	PT0005, PT0006	*WIKA* S-20	4 - 20 mA	0...6 bar(g)	±0.25% of span
	Pressure	PT0007, PT0008	*WIKA* S-20	4 - 20 mA	0...4 bar(g)	±0.25% of span
	Differential pressure	DPT0001	*WIKA* DPT-20	4 - 20 mA	−500... + 500 mbar	±0.25% of span

of 20%ethylene-glycol and water solution have been charged into the tank of the heating loop.

The IRIS setup was successfully commissioned to ensure the correct installation and operation of all the hardware of the system. The process variables were recorded until the steady-state operating conditions were reached. The results were compared with the requirements and specifications defined during the design phase.

5.1 Operation Sequence

An automated procedure has been implemented in the *IRIS* LabView program to control the start-up, operation and shut-down phases of the facility. The activation of the refrigerant loop is only possible if the heating and cooling loops have reached their prescribed operating conditions. The initial phase of the start-up process of the facility, thus, involves a series of steps to put in operation the heating and the cooling loops.

In the start-up sequence of the heating loop, the P2001 pump is turned on first to enable the circulation of the glycol-water mixture. Then, the H2001 electric heater is activated and the TICSA2002 control loop is initiated. The procedure ends once the set point temperature at the evaporator inlet (TT2001) is reached. At the same time, the operation of the cooling loop is initiated. First, the baffles installed at the outlet section of the wind tunnel are opened. Then, the F1001 fan is switched on and its speed control (FC1001) is activated until the air flow rate reaches the set point value. Finally, the air temperature controller (TCA1001) is activated and the electric H1001 heater warms up the airflow. The procedure ends when the air temperature at the condenser inlet (TT1001) is equal to the desired value.

Once the start-up procedures of both the heating and the cooling loop are terminated, the transport loop is activated. To allow for a safe operation of the compressor, the superheat controller (SHC0001) is enabled and the compressor starts operating only once the refrigerant pressure in the loop is above a set point value of 0.25 bar(g). When this condition is achieved, the PICSA0002 pressure controller is activated and the FIC0001 frequency inverter regulates the inlet pressure of the compressor to match the design value. The SHC0001 superheat control system remains active throughout the operation. While the refrigerant loop is running, the TICA2001 temperature controller of the heating loop is activated to maintain the TT2001 temperature constant and equal to the design set point value.

The shut-down procedure is essentially the reverse of the start-up procedure. Initially, the procedure to turn off the refrigerant loop is performed. First, the compressor is gradually slowed down. Then, all the controllers of the loop are disabled. Thereafter, the termination sequences of the heating loop and the cooling loop take place simultaneously. First, the heating sources and the associated controllers are switched off. Following a fixed cooldown interval, the flow rate is interrupted by switching off both the P2001 pump and the FC1001 fan.

5.2 Results

The commissioning of the setup has been executed to ensure that the design specifications of the refrigerant loop are met. The objective is to test the system when operating at the design values of evaporation and condensation pressure and temperature to achieve the design cooling capacity (Tab. 1). Preliminary tests have been conducted in advance to test the hardware, the software and the alarm system. The test campaign discloses some differences between the theoretical process variables specified during the design phase (Sec. 2) and those identified during the commissioning phase, as demonstrated in the following.

The P2001 pump, installed in the heating loop, operates at a constant rotational speed. This results in a fixed glycol-water volumetric flow rate of 1.44 m^3/h within the evaporator, which is higher than the value identified during the design phase. Therefore certain operating conditions have been adjusted to achieve the target value of cooling capacity of the evaporator (HX0002). Figure 3 shows the variation over time of the temperature values of the glycol-water flow in the heating loop, along with the refrigerant

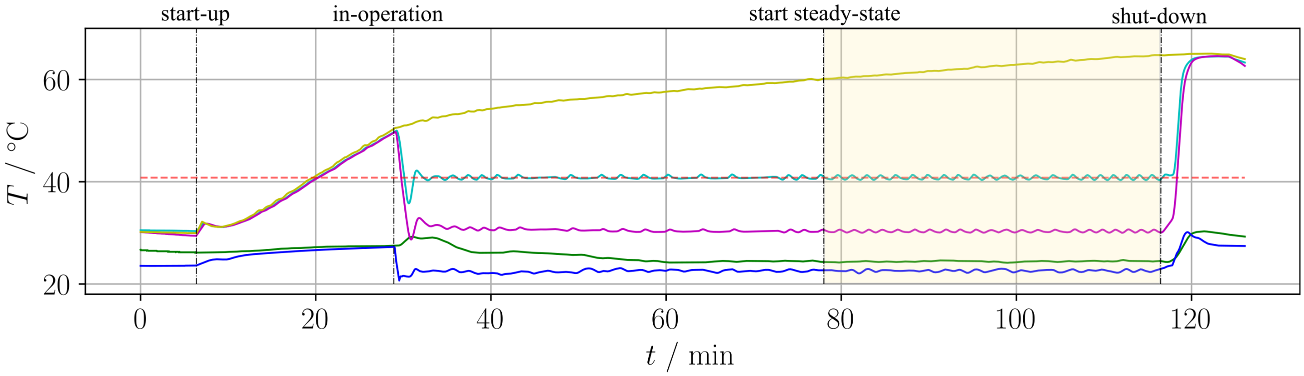

FIGURE 3: Temperature evolution over time recorded by the TT2003(—), TT2001 (—), and TT2002 (—) temperature transducers of the heating loop; and by the TT0010 (—), and TT0001 (—) temperature transducers of the refrigerant loop. Set point of the TICA2001 controller regulating the temperature monitored by the TT2001 temperature transducer (- -). The time interval highlighted with the coloured box indicates the period in which the process can be considered at steady-state.

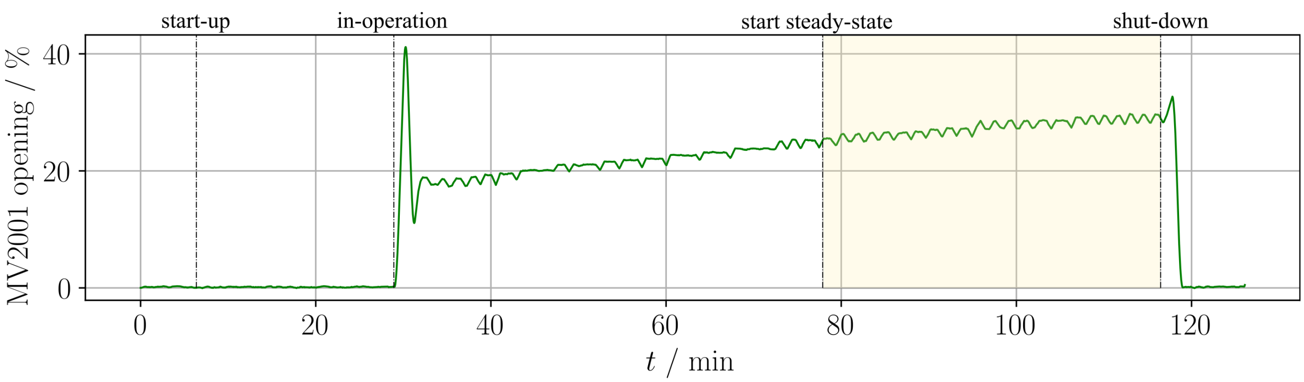

FIGURE 4: Evolution over time of the MV2001 mixing valve opening in the refrigerant loop. The time interval highlighted with the coloured box indicates the period in which the process can be considered at steady-state.

temperature upstream and downstream of the evaporator. When the TICSA2002 control is active, the heater turns off automatically once the set point value of temperature TT2003 is reached. However, preliminary tests have revealed that after some time, during steady-state operation, the temperature TT2003 starts rapidly decreasing. Although the heater turns on again, the thermal inertia of the hot water inside the tank is too high for a quick recovery of the delivery temperature of the heating loop. Consequently, the H2001 heater has been kept active throughout the entire test duration, ensuring that the temperature at the outlet of the tank (TT2003) constantly increases. During the start-up phase, the temperature of the glycol-water mixture increases linearly in all the different loop sections. Once the temperature TT2003 reaches the predefined value of 49 °C, the refrigerant loop starts operating since, in the cooling loop, the process variables have already reached steady-state conditions (Fig.5). After t = 29 min from the beginning of the test, the compressor turns on and the refrigerant starts circulating within the evaporator and absorbing heat from the glycol-water flow, whose temperatures TT22001 and TT2002 rapidly drop. From this moment, the TICA2001 controller is active, and the MV2001 valve opening is regulated to achieve the set point temperature TT2001 equal to 40.8 °C. This value is lower than the 45 °C predicted during the design phase since the glycol-water volumetric flow rate is higher than considered in the design phase. Figure 4 reports the evolution of the mixing valve opening during the test. Since the temperature upstream of the valve increases during the test and the volumetric flow rate of glycol-water circulating in the loop is constant, the valve opening increases linearly. The temperature TT2002 is kept close to the set point value by increasing the amount of fluid recirculated from C to B. However, the PID control mechanism causes oscillations in the valve regulation, which are propagated to all the temperature trends. The temperature of the refrigerant entering the evaporator (TT0010) does not undergo significant variations during the test, and its mean value is equal to 22.6 °C. The temperature at the outlet (TT0001) is regulated by the EEV0001 controller, which determines an optimal superheating degree of approximately 4 K. This variable reaches steady-state condition after about t = 78 min, where the amplitude of its oscillations remains within ±0.4% of the mean value until the shut-down phase is initiated. During the steady-state operation, the average pressure drop of the refrigerant and the water-glycol flow within the evaporator are equal to 1.4 kPa and 5.1 kPa, respectively. The IRIS setup has been kept running in steady-state conditions for approximately 38 min. Then the compressor is shut down, together with the H2001 heater. First, the temperatures in the loop rapidly increase, then, once the pump is turned off, they reach a steady condition and slowly decrease by passive cooling.

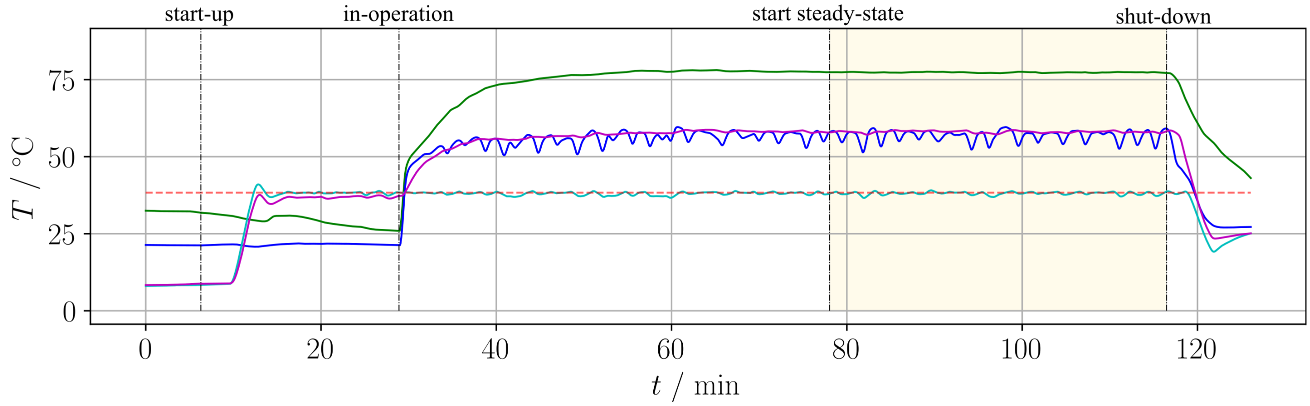

FIGURE 5: Temperature evolution over time recorded by the TT1001 (—), and TT1002 (—) temperature transducers mounted in the cooling loop; and the TT0006 (—), and TT0007 (—) temperature transducers installed in the refrigerant loop. Set point of the TCA1001 controller for the temperature monitored by the TT1001 temperature transducer (- -). The time interval highlighted with the coloured box indicates the period in which the process can be considered at steady-state.

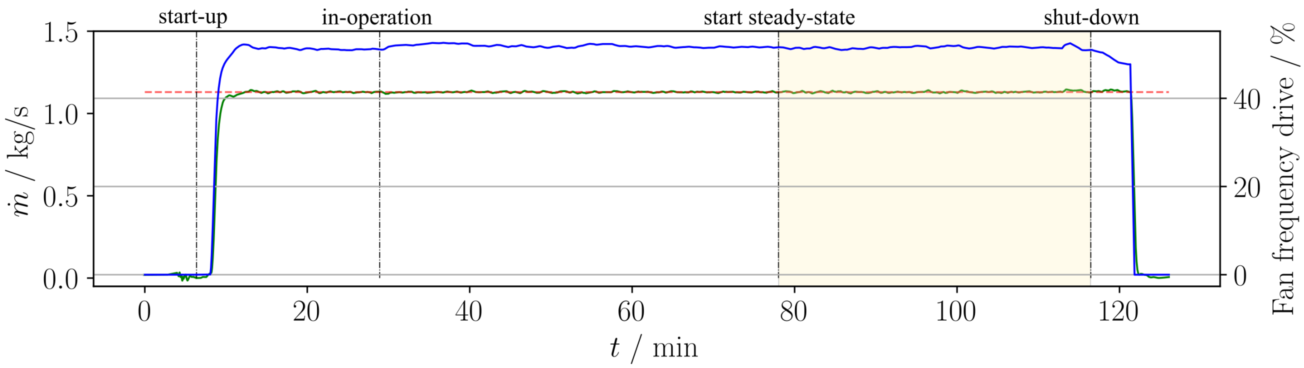

FIGURE 6: Left axis: evolution over time of the air mass flow rate recorded by the FT1001 flow transducer within the cooling loop (—). Set point of the FC1001 controller for the mass flow rate monitored by the FT1001 sensor (- -). Right axis: regulation of the adjustable-frequency drive of the FC1001 fan via the FC1001 controller during operation (—). The time interval highlighted with the coloured box indicates the period in which the process can be considered at steady-state.

Figure 5 shows the variation over time in the temperatures of the airflow and the refrigerant upstream and downstream of the condenser. Once the start-up of the loop is initiated, the F1001 fan is activated. Then, the H1001 heater is turned on and the TCA1001 control is activated. The temperature TT1001 of the air entering the condenser is regulated to be maintained at the set point value of the 38 °C. At the same time, the FC1001 flow control regulates the fan speed to allow for an air mass flow rate equal to the target value of 1.13 kg/s (Fig. 6). This value is lower than the 1.40 kg/s calculated during the preliminary design. During preliminary tests, it was observed that it was not possible to heat the inlet air temperature up to 40 °C when the environmental temperature was too low. The test was performed during winter, and the ambient air temperature was equal to 9 °C. During operation, the elements of the electric heater underwent overheating, causing a critical alarm and the immediate shutdown of the loop. Therefore, during the commissioning phase, the set point value of temperature TT1001 has been lowered to 38 °C. As a consequence, to comply with the design condensation pressure of 3.48 bar(g), the air mass flow rate necessary to cool down the refrigerant in the condenser has been reduced to 1.13 kg/s. The average air temperature TT1002 downstream of the condenser during steady-state operation is 58 °C. The recorded values of the airflow temperature present oscillations in their trend. In particular, the fluctuations are stronger downstream of the condenser (TT1002) since the sensor was mounted closer to the heat exchanger outlet, where the flow may not be well mixed yet. Despite this, oscillations remain in an acceptable range, the control system of this loop could be improved by controlling the inlet temperature of the airflow to achieve the desired condensation pressure. In this way, the two loops would be interconnected and the manual tuning of the inlet temperature would not be necessary. The refrigerant temperatures upstream (TT0006) and downstream (TT0007) of the condenser exhibit a smooth trend in the steady-state region. Their mean values are respectively equal to 77 °C and 56 °C. The pressure drops across the condenser recorded during steady-state operation are 0.46 bar on the refrigerant side, and 102 Pa on the air side. Once the shut-down process starts, first the heater is turned off and the fan keeps operating for a few minutes to allow for a rapid cooling of the loop components.

Figure 7 reports the evolution of the refrigerant pressure upstream (PT0001) and downstream (PT0005) of the compressor during the test. As soon as the compressor turns on, the FIC0001 control is activated. It regulates the compressor frequency to meet

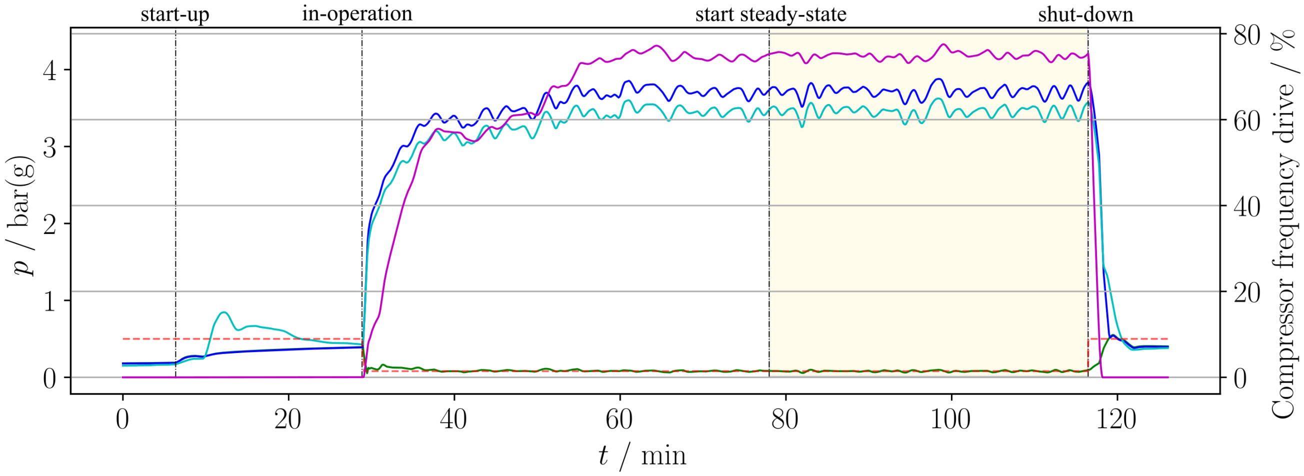

FIGURE 7: Left axis: pressure evolution over time recorded by the PT0001(—), PT0005 (—), and PT0006 (—) pressure transducers in the refrigerant loop. Set point of the PICSA0002 controller for the pressure recorded by the PT0001 sensor (- -). Right axis: regulation of the C0001 compressor frequency drive via the FIC0001 controller (—). The time interval highlighted with the coloured box indicates the period in which the process can be considered at steady-state.

the set point value of 0.08 bar(g) at the compressor suction port. Downstream of the compressor, the flow pressure reaches a steady state value of 3.7 bar(g). This value is higher than the design condensation pressure of 3.48 bar(g) at the inlet of the condenser (PT0006) due to the pressure losses in the hose connecting the compressor outlet and the condenser. Finally, once the shut-down is initiated, the compressor is the first component to be turned off, and the pressure of the refrigerant within the loop rapidly decreases.

6. SYSTEM PERFORMANCE AND UNCERTAINTY QUANTIFICATION

The analysis of the Type A uncertainty associated with the measurements using statical analysis has not been performed because of the oscillatory patterns characterizing the trends over time of the system process flow variables. Only the Type B uncertainty associated with the manufacturer-certified accuracy of the sensors has been considered. These values are reported in Tab. 4.

The performance of a refrigeration system is expressed in terms of COP, defined as the ratio between the VCC system cooling capacity and the power demand of the compressor

$$COP = \frac{\dot{Q}_{\mathrm{eva}}}{\dot{W}_{\mathrm{compr}}}. \tag{1}$$

Since the IRIS setup has not been equipped with a flow transducer to measure the refrigerant mass flow rate within the circuit, the heat duty of both the evaporator and the condenser has been respectively determined from the energy balance on the water-glycol and the airflow stream

$$\dot{Q}_{\mathrm{eva}} = \rho_{\mathrm{g\text{-}w}} \dot{V}_{\mathrm{g\text{-}w}} c_{p_{\mathrm{g\text{-}w}}} (T_{2001} - T_{2002}), \tag{2}$$

$$\dot{Q}_{\mathrm{cond}} = \rho_{\mathrm{a}} \dot{V}_{\mathrm{a}} c_{p_{\mathrm{a}}} (T_{1002} - T_{1001}). \tag{3}$$

Given the steady-state process variables of both loops, the density of the fluid (ρ) and the heat capacity at constant pressure (c_p) have been calculated using a well-assessed computer program [10]. In steady-state operating conditions, the evaporator cooling duty is equal to 17.88 ± 0.8 kW. The heat load of the condenser corresponds to 22.50 ± 0.25 kW.

The refrigerant loop is not equipped with a transducer to measure the refrigerant mass flow rate. Therefore, this quantity has been estimated as

$$\dot{m}_{\mathrm{refr}} = \frac{\dot{Q}_{\mathrm{cond}}}{\Delta h_{\mathrm{cond}}} \tag{4}$$

where Δh_{cond} is the difference of the enthalpy values calculated at the state points 3 and 4, respectively upstream and downstream of the condenser (Fig. 1). The resulting average value of refrigerant mass flow rate is equal to 0.12 kg/s, 12% higher than the value estimated in the design phase (Tab. 2).

The mechanical power transferred to the fluid in the compressor is calculated as

$$\dot{W}_{\mathrm{compr}} = \dot{m}_{\mathrm{refr}} \Delta h_{\mathrm{compr}}, \tag{5}$$

where $\Delta h_{\mathrm{compr}}$ is the enthalpy difference across the compressor. The compressor power is estimated to be equal to 4.75 ± 1 kW. Therefore, the corresponding system COP is equal to 3.76 ± 0.48. The uncertainty associated with these variables, which are a function of measured quantities, has been calculated recurring to the law of error propagation [15] with a 95% confidence interval.

Table 5 lists the mean values of temperature and pressure of each state point of the refrigerant loop of the IRIS setup recorded during steady-state operations, as well as the estimates for the same quantities calculated during the design phase. Figure 8 shows the T-s diagrams of the thermodynamic cycle of the IRIS setup based on the process variables measured during the commissioning and those calculated during the design phase.

The comparison shows that i) the system can operate at temperature levels which are very close to the design conditions, ii) the pressure drops within the heat exchangers have been underestimated during the design phase, especially in the condenser where the refrigerant pressure drop is 15 times higher than that at design point, iii) during the design phase, the pressure drop of 0.25 bar

TABLE 5: Comparison of temperature and pressure values of the main state points of the IRIS setup refrigeration loop resulting from preliminary design calculations and the commissioning. The state points refer to the P&ID in Fig. 1.

State point	Design conditions		Test conditions	
	T / °C	p / bar	T / °C	p / bar
1	25	1.08	24.4	1.09
2	80.18	4.48	79.5	4.70
3	80.18	4.48	77.3	4.45
4	60.76	4.45	56.8	4.0
5	20	1.08	22.6	1.15

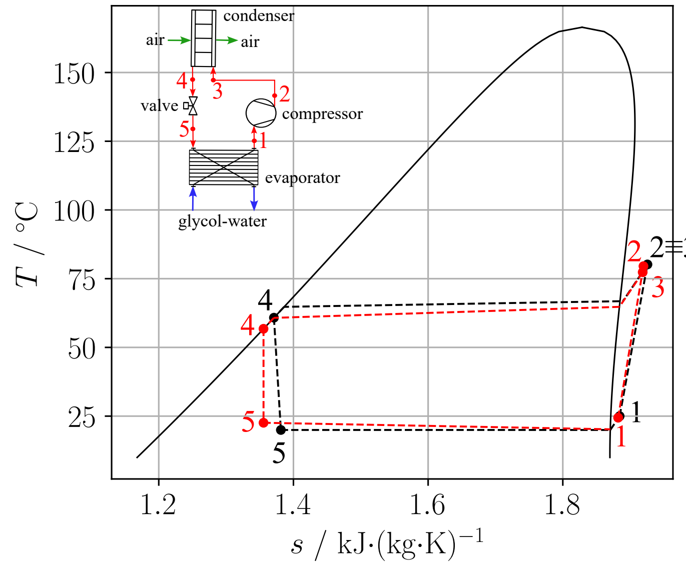

FIGURE 8: T-s diagram of the IRIS setup thermodynamic processes within the refrigeration loop. Comparison of the process variables estimated during the design phase (- -), and the commissioning phase (- -).

recorded within the hose connecting the compressor outlet and the condenser has been neglected. In reality, this negatively impacts the compressor power consumption which slightly increases to keep the design value of condensation pressure. At steady-state operating conditions, the evaporator cooling duty is higher than the one calculated during the design, therefore the COP of the IRIS setup is 4% higher than the design value.

7. CONCLUSIONS AND FUTURE WORK

This work documents the design and the commissioning of the IRIS setup. The purpose of this facility is to test the performance of Vapour Compression Cycle devices for aircraft Environmental Control Systems. The experimental data will be used to validate the *in-house* numerical tools developed for system and components simulation and optimization of VCC systems. A single balance of plant realizes a single-stage compression refrigeration cycle incorporating two test sections: one for the volumetric compressor and another for the air-cooled condenser. A mixture of 20% ethylene-glycol and water warmed up in an independent loop, is used as heat source for the refrigerant within the evaporator. The design working fluid is R-1233zd(E). The design cooling capacity of the system is 15.5 kW.

The facility was successfully commissioned. The hardware and the control system were correctly tested throughout the operation of the facility. Data of the process flow variables in each loop of the setup were recorded during the start-up, operation and shut-down procedures of the setup. The facility was continuously operating in steady-state for about 40 min, proving that the IRIS can operate under the design conditions, and the desired inlet conditions for both test sections of the setup can be achieved. The average values of inlet temperature and pressure at the compressor suction port are respectively equal to 22.6 °C and 0.08 bar(g). The mean value of condensation pressure corresponds to 3.48 bar(g). The system cooling capacity is slightly higher than the value calculated at design condition and it is equal to 17.88 ± 0.8 kW. This positively affects the COP of the IRIS setup which increases by 4% with respect to the value of efficiency estimated for the design point.

Future experimental tests are planned to evaluate the performance of the IRIS setup and its components when operating under different conditions than the design point. To this purpose, the evaporator and the condensation pressure of the refrigerant loop can be adjusted by varying the settings of the heating and cooling loops. The research will aim to characterize the volumetric compressor efficiency at various compression ratios and refrigerant mass flow rates. Additionally, the condenser test section will be further instrumented with the installation of thermocouple rakes. The idea is to assess the condenser performance, in terms of effectiveness and pressure drop, for various combinations of inlet thermodynamic conditions, and mass flow rate of both refrigerant and air streams.

ACKNOWLEDGMENTS

The authors gratefully acknowledge the precious technical expertise and contribution of M. van der Helm of RBK group during the detailed design of the IRIS setup. The authors are also grateful to L. van Luijk of DEMO for his valuable support during the design and the realization of the cooling loop of the IRIS setup. Finally, the authors are thankful to R. de Groot and G.J.M.A. Berends of Carya Automatisering for their meticulous efforts in the IRIS software implementation. This research is supported by Aeronamic BV, by the Applied and Engineering Sciences Division (TTW) of the Dutch Organization for Scientific Research (NWO) via the Technology Program of the Ministry of Economic Affairs of the Netherlands (Grant No. 17091).

REFERENCES

[1] ICAO. "Emissions from fuel used for international aviation and maritime transport." Technical report no. International Civil Aviation Organization, Dubai, United Arab Emirates. 2023.

[2] Sinnet, Mike. "787 No-bleed systems: saving fuel and enhancing operational efficiencies." Technical report no. Boeing. 2007.

[3] Zaporozhets, Oleksandr, Isaienko, Volodymyr and Synylo, Kateryna. "PARE preliminary analysis of ACARE FlightPath 2050 environmental impact goals." *CEAS Aeronautical Journal* Vol. 12 No. 3 (2021): pp. 653–667. DOI 10.1007/s13272-021-00525-7.

[4] Chowdhury, Shafayat Hasan, Ali, Fakhre and Jennions, Ian K. "Development of a Novel Ground Test Facility for Aircraft Environmental Control System." *Journal of Thermal Science and Engineering Applications* Vol. 15 No. 8 (2023). DOI 10.1115/1.4062553.

[5] Documentation Simulink. "Simulation and Model-Based Design." (2020).

[6] Mancin, Simone, Zilio, Claudio, Righetti, Giulia and Rossetto, Luisa. "Mini Vapor Cycle System for high density electronic cooling applications." *International Journal of Refrigeration* Vol. 36 No. 4 (2013): pp. 1191–1202. DOI 10.1016/J.IJREFRIG.2012.12.008.

[7] ARP292. "Air Conditioning Helicopter General Requirements." *SAE International* (2014)DOI 10.4271/ARP292.

[8] Ascione, Federica, De Servi, Carlo Maria, Meijer, Onno, Pommé, Vincent and Colonna, Piero. "Assessment of an Inverse Organic Rankine cycle system for the ECS of a large rotorcraft adopting a high-speed centrifugal compressor and a low GWP refrigerant." Technical University of Munich (ed.). *Proceedings of the 6th International Seminar on ORC Power Systems*. 2021. Technical University of Munich. DOI 10.14459/2021mp1633127.

[9] Heath, Eric A. "Amendment to the Montreal Protocol on Substances that Deplete the Ozone Layer (Kigali Amendment)." *International Legal Materials* Vol. 56 (2017): pp. 193–205.

[10] Lemmon, E. W., Bell, I. H., Huber, M. L. and McLinder, M. O. "NIST Standard Reference Database 23: Reference Fluid Thermodynamic and Transport Properties-REFPROP, Version 10.0, National Institute of Standards and Technology." (2018). DOI 10.18434/T4/1502528.

[11] ANSI/ASHRAE Standard 34. "ASHRAE Standard 34-2022 - Designation and Safety Classification of Refrigerants." (2022).

[12] American National Standard. "ANSI/ISA-5.1-2009, Instrumentation symbols and identification." (2009).

[13] ANSI/ASHRAE Standard 41.2-2022. "Standard methods for air velocity and airflow measurement." (2022).

[14] DIN EN 378-2. "Refrigerating systems and heat pumps - Safety and environmental requirements - Part 2: Design, construction, testing, marking and documentation." (2018).

[15] ISO/IEC Guide 98-3:2008. "Uncertainty of measurement. Part 3: Guide to the expression of uncertainty in measurement." (2008).